Effects of the propagation of ultrasound on linear longitudinal conductivity in degenerate semiconductors

1981 J. Phys. C: Solid State Phys. 14 3005

(http://iopscience.iop.org/0022-3719/14/21/017)

J. Phys. C: Solid State Phys., **14** (1981) 3005–3014. Printed in Great Britain

Effects of the propagation of ultrasound on linear longitudinal conductivity in degenerate semiconductors†

Chhi-Chong Wu‡ and Jensan Tsai§

‡ Department of Applied Mathematics, National Chiao Tung University, Hsinchu, Taiwan, China

§ Institute of Nuclear Science, National Tsing Hua University, Hsinchu, Taiwan, China

Received 21 January 1981

Abstract. The effect of the propagation of ultrasound at an angle θ relative to the direction of a DC magnetic field $\boldsymbol{B}$ in a degenerate semiconductor such as n-type InSb is investigated by using a quantum treatment which is valid at high frequencies and in strong magnetic fields. It is found that the real and imaginary parts of the linear longitudinal conductivity oscillate with the DC magnetic field when ultrasound propagates along the field for both parabolic and nonparabolic band structures. However, if the angle θ is different from zero, these oscillations diminish for the nonparabolic band structure, and no oscillations can be observed for the parabolic band structure.

1. Introduction

The magnetic field dependence and the frequency dependence of the conductivity tensors in semimetals and semiconductors have been investigated by several authors (Quinn 1964, Wu and Tsai 1973, Wu *et al* 1973, Arora and Miller 1974, Andreev 1979, Matulis and Chenis 1979, V'yurkov and Domnin 1979, Fishchuk and Rudko 1980, Wu and Tsai 1980). Several experiments (Nill and McWhorter 1966, Hafele *et al* 1971) in n-type InSb on the magnetoacoustic phenomena for ultrasound propagating parallel to a DC magnetic field have revealed a magnetic field dependence over a wide range of field strengths. The magnetoacoustic effects in semiconductors could be explained by the magnetic field dependence of the linear longitudinal conductivity tensor (Spector 1966, Nill and McWhorter 1966). The degenerate electron gas model has been extremely useful in study of the electronic properties of semimetals and degenerate semiconductors in the presence of a uniform DC magnetic field (Wu and Tsai 1972, 1973, 1974). When the ultrasound is propagating parallel to the DC magnetic field, the effect of nonparabolicity and the quantum effect of oscillations will appear much more important in the strong magnetic field region (Sharma and Phadke 1972, Wu and Tsai 1972, 1974, Sutherland and Spector 1978). These magnetoacoustic phenomena in semiconductors are dominated by the linear longitudinal conductivity, because the longitudinal field is important when the interaction of ultrasound with conduction electrons in semiconductors is by way of either the piezoelectric or deformation potential coupling mechanisms (Spector 1966). Lifshitz *et al* (1966) obtained values directly for the energy relaxation

† Partially supported by National Science Council of China in Taiwan.

0022-3719/81/213005 + 10 $01.50

time by measuring the real and imaginary parts of the complex conductivity at 250 and 400 kHz. They concluded that piezoelectric scattering is predominantly responsible for the energy relaxation and that deformation potential scattering contributes relatively little to the energy relaxation. In our previous work on nondegenerate semiconductors (Wu and Tsai 1980), it has been shown that the linear longitudinal conductivity depends strongly on the DC magnetic field, the sound frequency, and the direction of the propagation of ultrasound relative to that of the field. For the ultrasound propagating parallel to the DC magnetic field in degenerate semiconductors, the linear longitudinal conductivity for both parabolic and nonparabolic models depends upon the field and its real part oscillates more rapidly and saliently than its imaginary part (Wu *et al* 1973). We shall now study the effect of varying the angle between the direction of ultrasonic propagation and that of the magnetic field on the linear longitudinal conductivity for parabolic and nonparabolic band structures in degenerate semiconductors such as n-type InSb. We also make the following assumptions.

(i) For a degenerate semiconductor, the distribution function of electrons is represented by the Fermi–Dirac statistics. The interesting temperature is very near absolute zero.

(ii) We are interested in the high-frequency region with $|\boldsymbol{q}|\, l \gg 1$, where $\boldsymbol{q}$ is the ultrasonic wavevector and l is the electron mean free path; the effect of collisions can be neglected and we do not take into account the effect of the electron relaxation time in our present case.

In § 2, we perform the calculation of the linear longitudinal conductivity for parabolic and nonparabolic bands in the presence of a DC magnetic field $\boldsymbol{B}$ with which the ultrasonic wavevector $\boldsymbol{q}$ propagates along an angle θ. In § 3 some numerical results for the real and imaginary parts of the linear longitudinal conductivity are presented by taking n-type InSb as an example. We also give a brief discussion.

2. Linear longitudinal conductivity tensors for parabolic and nonparabolic band structures

In the parabolic model, the energy eigenvalue equation for electrons in a uniform DC magnetic field $\boldsymbol{B}$ directed along the z axis is

$$H_0\psi_{kn} \equiv (1/2m^*)\,[p_x^2 + (p_y - eBx/c)^2 + p_z^2]\;\psi_{kn} = E_{kn}\psi_{kn}, \tag{1}$$

where m^* is the effective mass of electrons at the minimum of the conduction band and we have used the Landau gauge for the vector potential $\boldsymbol{A}_0 = (0, Bx, 0)$. For the case of a nonparabolic model, the energy eigenvalue equation in the magnetic field directed along the z axis can be written as

$$H_0(1 + H_0/E_g)\;\psi_{kn} \equiv (1/2m^*)\,[p_x^2 + (p_y - eBx/c)^2 + p_z^2]\psi_{kn}$$
$$= E_{kn}\,(1 + E_{kn}/E_g)\;\psi_{kn}, \tag{2}$$

where E_g is the energy gap between the conduction and valence bands. The eigenfunctions for equations (1) and (2) will have the same representation which can be expressed by the Landau representation,

$$\psi_{kn} = \exp(\mathrm{i}k_y y + \mathrm{i}k_z z)\;\Phi_n[x - (\hbar c/eB)\;k_y] \tag{3}$$

where k_y and k_z are the y and z components of the electron wavevector $\boldsymbol{k}$, and $\Phi_n(x)$ is

the wavefunction for a simple harmonic oscillator. But the eigenvalues of equation (1) for a parabolic model are

$$E_{kn} = \hbar\omega_c(n + \tfrac{1}{2}) + \hbar^2 k_z^2/2m^* \tag{4}$$

while the eigenvalues of equation (2) for a nonparabolic model are

$$E_{kn} = -\tfrac{1}{2}E_g\{1 - [1 + (4/E_g)\,((n + \tfrac{1}{2})\,\hbar\omega_c + \hbar^2 k_z^2/2m^*)]^{1/2}\}, \tag{5}$$

where $\omega_c = |e|B/m^*c$ is the cyclotron frequency of electrons. Equation (4) gives the eigenvalues for a one-band model and equation (5) gives the eigenvalues of the conduction band for a two-band model. When $(n + \frac{1}{2})\,\hbar\omega_c + \hbar^2 k_z^2/2m^* \ll E_g$ equation (5) can be reduced to that obtained using the parabolic model for the band structure as shown in equation (4).

In our present case, it is assumed that the principal electron–phonon interaction in semiconductors is by way of either the piezoelectric or deformation potential coupling mechanisms. Since the transverse electric fields induced by the ultrasound in semiconductors are down by a factor of $(v_s/c)^2$ from the longitudinal electric fields (Spector 1966), where v_s is the velocity of sound, the interaction of the charge carriers and the piezoelectric or deformation potential fields is known to be strongest for longitudinal electric fields. Consequently, the only component of the linear conductivity tensors of interest is σ_{zz}. Following the same method of quantum treatment as the previous paper (Wu *et al* 1973), the linear longitudinal conductivity can be obtained as

$$\sigma_{zz}(\boldsymbol{q}, \omega) = \frac{\omega_p^{*2}}{4\pi i\omega n_0}\left[\sum_{k,n} f_{kn} - \frac{\hbar^2}{4m^*}\sum_{k,n,n'}\frac{(f_{kn} - f_{k+q,n'})}{E_{k+q,n'} - E_{kn} - \hbar\omega} \times (2k_z + q\cos\theta)^2\,|M_{n,n}(q\sin\theta)|^2\right] \tag{6}$$

for the parabolic model, and

$$\sigma_{zz}(\boldsymbol{q}, \omega) = \frac{\omega_p^{*2}}{4\pi i\omega n_0}\left[\sum_{k,n} f_{kn}\theta_{kn} - \frac{\hbar^2}{4m^*}\sum_{k,n,n'}\frac{(f_{kn} - f_{k+q,n'})\,\theta_{kn}\theta_{k+q,n'}}{E_{k+q,n'} - E_{kn} - \hbar\omega} \times (2k_z + q\cos\theta)^2\,|M_{n'n}(q\sin\theta)|^2\right] \tag{7}$$

for the nonparabolic model. Here n_0 is the electron density at $\boldsymbol{B} = 0$, $\omega_p^* = (4\pi n_0 e^2/m^*)^{1/2}$ is the plasma frequency of the electron with the effective mass m^*, ω is the frequency of the ultrasound, f_{kn} is the Fermi–Dirac distribution for electrons in degenerate semiconductors, θ is the angle between the ultrasonic wavevector $\boldsymbol{q}$ and the DC magnetic field $\boldsymbol{B}$, and θ_{kn} is given by

$$\theta_{kn} = (1 + 2E_{kn}/E_g)^{-1}. \tag{8}$$

The function $|M_{n'n}(q\sin\theta)|^2$ is defined by

$$|M_{n'n}(q\sin\theta)|^2 = (n!/n'!)\,(\tfrac{1}{2}L^2q^2\sin^2\theta)^{n'-n}\exp(-\tfrac{1}{2}L^2q^2\sin^2\theta) \times [L_n^{n'-n}(\tfrac{1}{2}L^2q^2\sin^2\theta)]^2 \qquad \text{for } n' \geqslant n \tag{9a}$$

and

$$|M_{n'n}(q\sin\theta)|^2 = (n'!/n!)\,(\tfrac{1}{2}L^2q^2\sin^2\theta)^{n-n'}\exp(-\tfrac{1}{2}L^2q^2\sin^2\theta) \times [L_{n'}^{n-n'}(\tfrac{1}{2}L^2q^2\sin^2\theta)]^2 \qquad \text{for } n' < n, \tag{9b}$$

where $L = (\hbar/m^*\omega_c)^{1/2}$ is the classical radius of the lowest Landau level and $L_l^n(x)$ is the associated Laguerre polynomial.

3. Numerical results and discussion

Since $(\hbar k_{z\max})^2/2m^* \ll E_g$ at the very low temperature limit in which we are interested, equation (5) can be expanded as

$$E_{kn} \simeq -\tfrac{1}{2}E_g + \tfrac{1}{2}E_g a_n + \hbar^2 k_z^2/2m^* a_n \tag{10}$$

with

$$a_n = [1 + (4\hbar\omega_c/E_g)(n + \tfrac{1}{2})]^{1/2}. \tag{11}$$

We now shall improve our numerical calculations for the nonparabolic band structure by using $\theta_{kn} = [a_n(1 + \hbar^2 k_z^2/m^* a_n^2 E_g)]^{-1}$ instead of the previously used value (Wu and Tsai 1972, Wu *et al* 1973) $\theta_{kn} \simeq a_n^{-1}$, which is valid in strong magnetic fields.

As a numerical example, we consider the linear longitudinal conductivity in n-type InSb at high frequencies and very low temperature limit. The relevant values of physical parameters for degenerate n-type InSb are shown in table 1 and $v_s = 4 \times 10^5$ cm s^{-1}.

Table 1. Physical parameters for n-type InSb.

n_0 (cm^{-3})	m^*†	E_g (eV)	E_F (eV)
3×10^{18}	$0.029m_0$	0.38	0.2616
10^{19}	$0.039m_0$	0.50	0.4340

† Note that m_0 is the mass of a free electron.

The real and imaginary parts of the linear longitudinal conductivity σ_{zz} are plotted as a function of DC magnetic field B for the nonparabolic band structure with different angles θ and different electron densities n_0 as shown in figures 1 and 2. It can be seen that both real and imaginary parts of σ_{zz} oscillate with the DC magnetic field at $\theta = 0°$. However, when the direction of the ultrasonic propagation is not the same as that of the DC magnetic field, oscillations of the imaginary part will diminish as shown in figure 2. When the electron density increases, both oscillations of the real and imaginary parts will become insignificant. Furthermore, both real and imaginary parts of σ_{zz} will abruptly increase to very large values when the DC magnetic field is down to the intermediate region. For the parabolic band structure as shown in figures 3 and 4, it can be seen that both real and imaginary parts of σ_{zz} oscillate with the DC magnetic field when ultrasound propagates along with the direction of the field $\boldsymbol{B}$, but no oscillations can be observed when the angle θ is different from zero. These oscillations can be interpreted as the so-called 'giant quantum oscillations' (Gurevich *et al* 1961, Liu and Toxen 1965, Bass and Levinson 1965). These oscillations occur for degenerate semiconductors in which electrons obey Fermi–Dirac statistics when the sound wavevector $\boldsymbol{q}$ has a component along the DC magnetic field $\boldsymbol{B}$. When the angle θ increases, the component of $\boldsymbol{q}$ along the magnetic field is reduced, consequently the effect of oscillations diminishes. We also can see that the real part of σ_{zz} increases to large values, while the imaginary part will abruptly diminish to small values in the intermediate magnetic field region when $\theta =$

45°. This is different from that of the nonparabolic band structure as shown in figure 2. From these numerical results, it can be seen that the direction of ultrasonic propagation with respect to the DC magnetic field will affect the dependence of the linear longitudinal conductivity on the magnetic field and the model of energy band structures. In order to investigate more clearly the effect of the angle θ between the direction of ultrasonic propagation and that of the DC magnetic field upon the linear longitudinal conductivity,

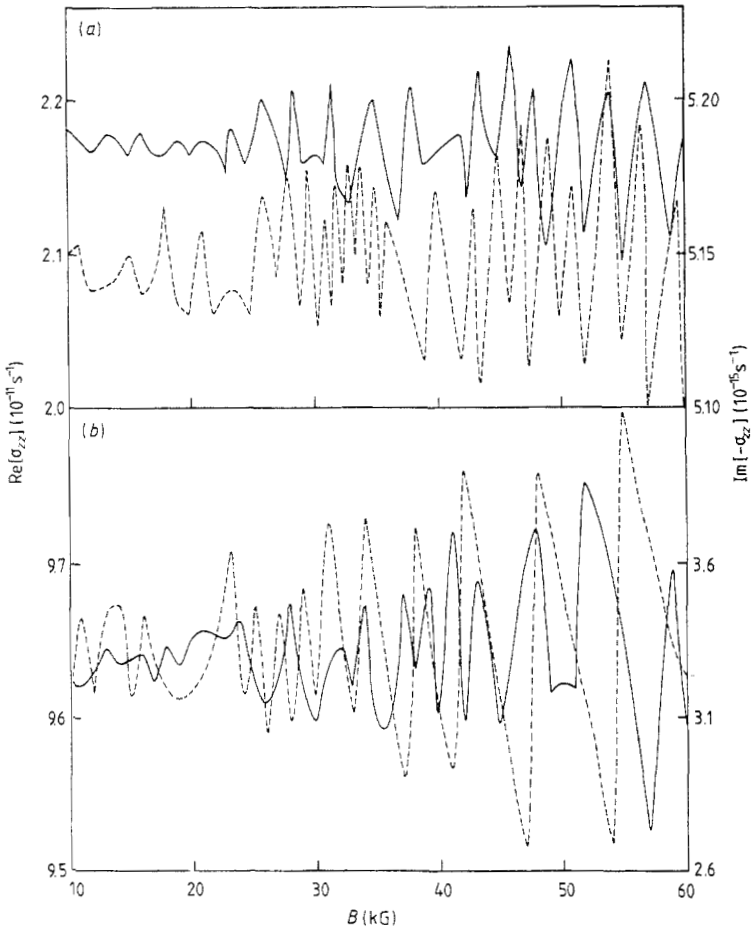

Figure 1. Real part (full curves) and imaginary part (broken curves) of the linear longitudinal conductivity σ_{zz} as a function of DC magnetic field B in n-type InSb for the nonparabolic band structure with $\theta = 0°$ at $\omega = 2 \times 10^{12}$ rad s^{-1}. (*a*) $n_0 = 3 \times 10^{18}$ cm^{-3}; (*b*) $n_0 = 10^{19}$ cm^{-3}.

we plot Re$[\sigma_{zz}]$ and Im$[-\sigma_{zz}]$ as a function of the angle θ as shown in figures 5 and 6 for electron density $n_0 \simeq 3 \times 10^{18}$ cm^{-3}. For the nonparabolic band structure shown in figure 5, Re$[\sigma_{zz}]$ has maxima and minima in the region excluding $\theta = 0°$ and $\theta = 90°$. These maxima and minima appear like spikes due to the degeneracy of the electron gas. As the angle θ approaches 90°, both real and imaginary parts of σ_{zz} will be diminished in the intermediate magnetic field region. However, in the strong magnetic field region, say

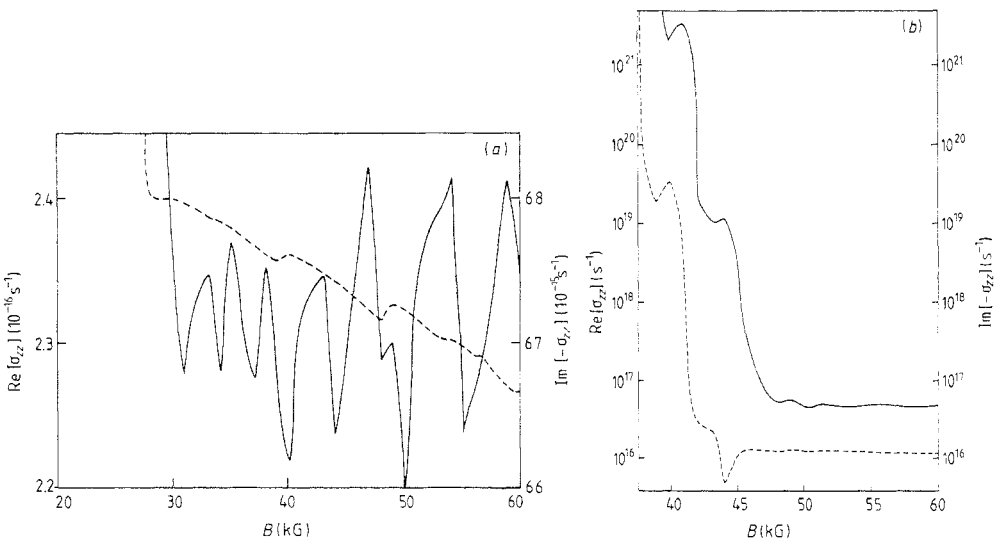

Figure 2. Real part (full curves) and imaginary part (broken curves) of the linear longitudinal conductivity σ_{zz} as a function of DC magnetic field B in n-type InSb for the nonparabolic band structure with $\theta = 45°$ at $\omega = 2 \times 10^{12}$ rad s^{-1}. (*a*) $n_0 = 3 \times 10^{18}$ cm^{-3}; (*b*) $n_0 = 10^{19}$ cm^{-3}.

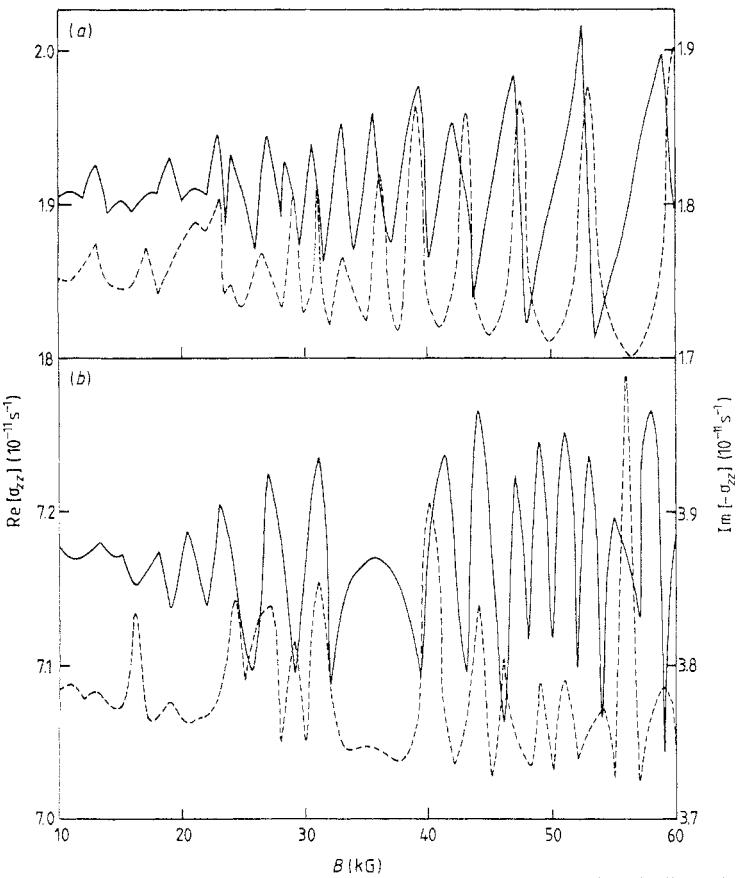

Figure 3. Real part (full curves) and imaginary part (broken curves) of the linear longitudinal conductivity σ_{zz} as a function of DC magnetic field B in n-type InSb for the parabolic band structure with $\theta = 0°$ at $\omega = 2 \times 10^{12}$ rad s^{-1}. (*a*) $n_0 = 3 \times 10^{18}$ cm^{-3}; (*b*) $n_0 = 10^{19}$ cm^{-3}.

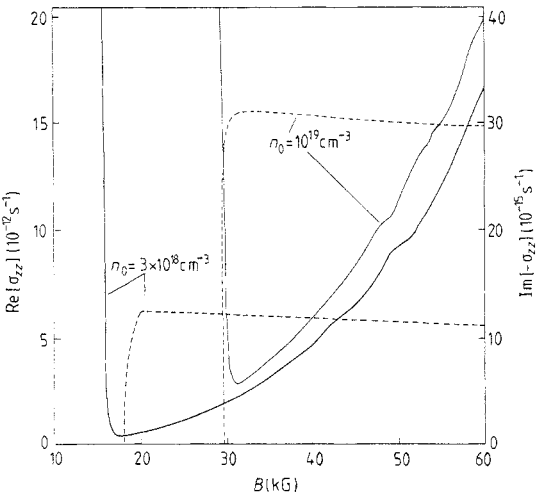

Figure 4. Real part (full curves) and imaginary part (broken curves) of the linear longitudinal conductivity σ_{zz} as a function of DC magnetic field B in n-type InSb for the parabolic band structure with $\theta = 45°$ at $\omega = 2 \times 10^{12}$ rad s^{-1}. (*a*) $n_0 = 3 \times 10^{18}$ cm^{-3}; (*b*) $n_0 = 10^{19}$ cm^{-3}.

$B = 40$ kG, the imaginary part of σ_{zz} can not be diminished when $\theta = 90°$. For the parabolic band structure shown in figure 6, it shows that the real part of σ_{zz} is diminished to zero at $\theta = 90°$, but the imaginary part of σ_{zz} can not vanish there. Consequently, it can be predicted that the absorption coefficient becomes insignificant at $\theta = 90°$. This result is the same as that for nondegenerate semiconductors (Wu and Tsai 1980) and in

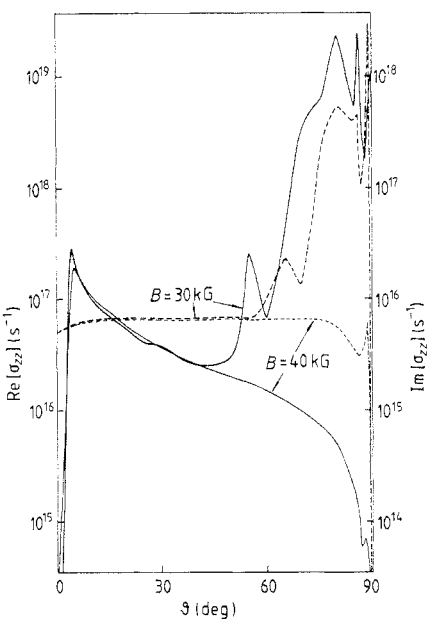

Figure 5. Real part (full curves) and imaginary part (broken curves) of the linear longitudinal conductivity σ_{zz} as a function of angle θ in n-type InSb for the nonparabolic band structure at $\omega = 2 \times 10^{12}$ rad s^{-1} with $n_0 = 3 \times 10^{18}$ cm^{-3}.

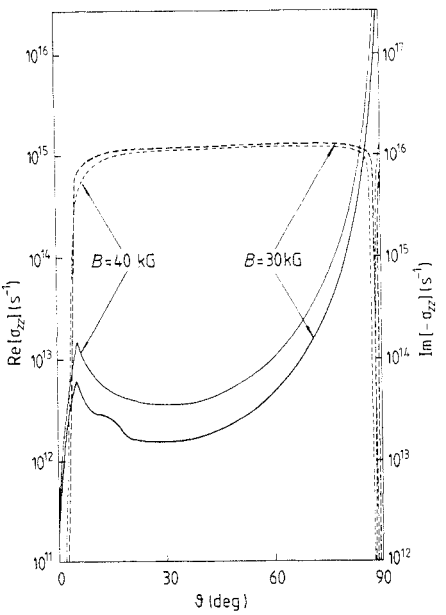

Figure 6. Real part (full curves) and imaginary part (broken curves) of the linear longitudinal conductivity σ_{zz} as a function of angle θ in n-type InSb for the parabolic band structure at $\omega = 2 \times 10^{12}$ rad s^{-1} with $n_0 = 3 \times 10^{18}$ cm^{-3}.

qualitative agreement with experimental results at high frequencies and in strong magnetic fields (Smith *et al* 1971). Next, we study the frequency dependence of the linear longitudinal conductivity for parabolic and nonparabolic band structures. In figure 7(*a*), we can see that both $\mathrm{Re}[\sigma_{zz}]$ and $\mathrm{Im}[\sigma_{zz}]$ decrease with increasing sound frequency ω for the nonparabolic band streucture at $\theta = 0°$. However, when the sound frequency is

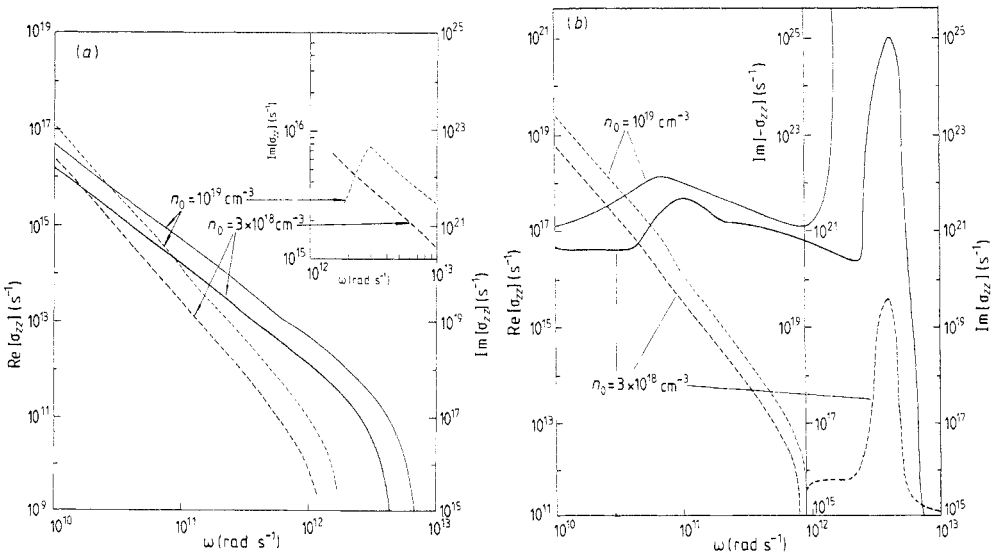

Figure 7. Real part (full curves) and imaginary part (broken curves) of the linear longitudinal conductivity σ_{zz} as a function of sound frequency ω in n-type InSb for the nonparabolic band structure at $B = 30$ kG. (*a*) $\theta = 0°$; (*b*) $\theta = 45°$.

above the microwave region ($\omega > 10^{12}$ rad s^{-1}), Im[σ_{zz}] will abruptly be changed to the negative values. When $\theta = 45°$ shown in figure 7(*b*), we can see that both Re[σ_{zz}] and Im[$-\sigma_{zz}$] have a maximum in the microwave region for $n_0 = 3 \times 10^{18}$ cm^{-3}. As the electron density increases, these maxima will disappear and become very large. We also plot Re[σ_{zz}] and Im[σ_{zz}] as a function of sound frequency ω for the parabolic band structure in figures 8(*a*) and 8(*b*). When the direction of propagation of ultrasound is

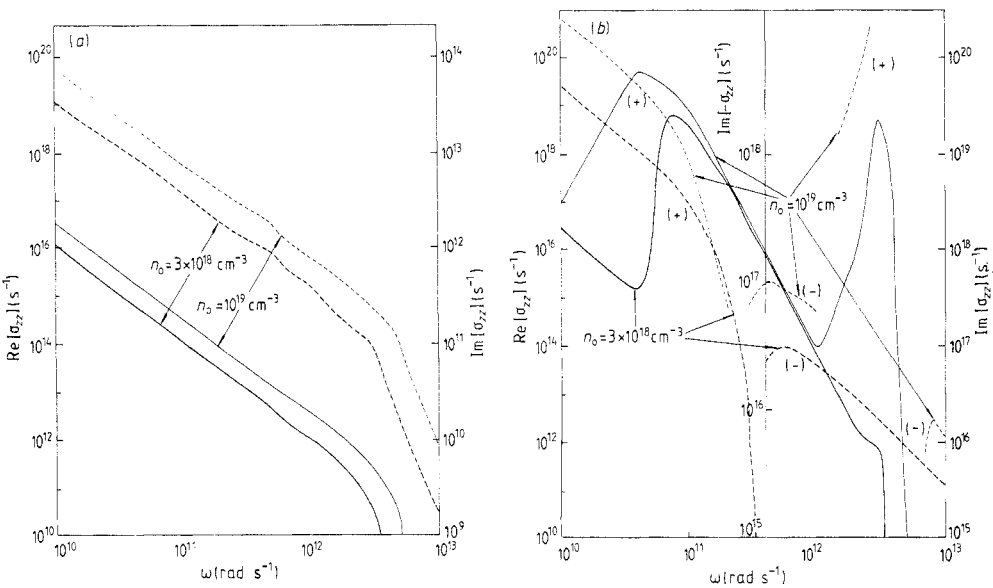

Figure 8. Real part (full curves) and imaginary part (broken curves) of the linear longitudinal conductivity σ_{zz} as a function of sound frequency ω in n-type InSb for the parabolic band structure at $B = 30$ kG. (*a*) $\theta = 0°$; (*b*) $\theta = 45°$.

parallel to the DC magnetic field, both Re[σ_{zz}] and Im[σ_{zz}] decrease with increasing sound frequency, but the imaginary part of σ_{zz} does not change its sign above the microwave region. However, when the angle θ is different from zero, some maxima and minima of Re[σ_{zz}] can be observed and discontinuities exist in and above the microwave region. These discontinuities are due to the fact that the linear longitudinal conductivity may have singularities of purely quantum origin related to the degeneracy of the electron gas (Bakanas 1970). Since the absorption coefficient due to the interaction between the ultrasound and conduction electrons is proportional to Re[σ_{zz}] and the change in sound velocity due to the interaction between the ultrasound and conduction electrons is proportional to $(1 - (4\pi \text{ Im}[\sigma_{zz}]/\omega\varepsilon))$ (Spector 1966), therefore the magnetoacoustic phenomena in semiconductors depend strongly on both real and imaginary parts of the linear longitudinal conductivity. We predict that the absorption coefficient and change in sound velocity oscillate with the DC magnetic field only for the nonparabolic band structure when the angle θ is not zero.

References

Andreev S P 1979 *Zh. Eksp. Teor. Fiz.* **77** 1046–57 (Engl. Transl. 1979 *Sov. Phys.–JETP* **50** 526–32)
Arora V K and Miller S C 1974 *Phys. Rev.* B **10** 688–97

Bakanas R K 1970 *Fiz. Tverd. Tela* **12** 3408–12 (Engl. Transl. 1971 *Sov. Phys.–Solid State* **12** 2769–73)
Bass F G and Levinson I B 1965 *Zh. Eksp. Teor. Fiz.* **49** 914–24 (Engl. Transl. 1966 *Sov. Phys.–JETP* **22** 635–42)
Fishchuk I I and Rudko V N 1980 *J. Phys. C: Solid State Phys.* **13** 2703–13
Gurevich V L, Skobov V G and Firsov Yu A 1961 *Zh. Eksp. Teor. Fiz.* **40** 786–91 (Engl. Transl. 1961 *Sov. Phys.–JETP* **13** 552–5)
Hafele H G, Grisar R, Irslinger C, Wachernig H, Smith S D, Dennis R B and Wherrett B S 1971 *J. Phys. C: Solid State Phys.* **4** 2637–49
Lifshitz T M, Oleinikov A Ya and Shulman A Ya 1966 *Phys. Status Solidi* **14** 511–6
Liu S H and Toxen A M 1965 *Phys. Rev.* **138** A 487–93
Matulis A and Chenis A 1979 *Zh. Eksp. Teor. Fiz.* **77** 1134–43 (Engl. Transl. 1979 *Sov. Phys.–JETP* **50** 572–6)
Nill K W and McWhorter A L 1966 *J. Phys. Soc. Japan* Suppl.**21** 755–9
Quinn J J 1964 *Phys. Rev.* **135** A 181–5
Sharma S and Phadke U P 1972 *Phys. Rev. Lett.* **29** 272–4
Smith W D, Miller J G, Sundfors R K and Bolef D I 1971 *J. Appl. Phys.* **42** 2579–84
Spector H N 1966 *Solid State Phys.* **19** 291–361 (New York: Academic Press)
Sutherland F R and Spector H N 1978 *Phys. Rev.* B **17** 2728–32, 2733–9
Wu C C and Tsai J 1972 *J. Phys. C: Solid State Phys.* **5** 2419–26
—— 1973 *Appl. Phys. Lett.* **22** 297–8
—— 1974 *Phys. Rev.* B **9** 3337–46
—— 1980 *J. Phys. C: Solid State Phys.* **13** 3253–9
Wu C C, Tsai J and Spector H N 1973 *Phys. Rev.* B**7** 3836–42
V'yurkov V V and Domnin P V 1979 *Fix. Tekh. Poluprov.* **13** 1951–7 (Engl. Transl. 1979 *Sov. Phys.–Semicond.* **13** 1137–40)